

Analysis of Changes in Hydration Products During Solidification/Stabilization Process of Heavy Metals in the Presence of Magnesium Potassium Phosphate Cement

Shucong Zhen^{1*}, Xiaohui Dong¹, Gloria Appiah-Sefah², Mei Pan¹ and Dekun Zhou¹

¹*School of Architecture and Construction, Yancheng Institute of Technology,
Yancheng 224051, P.R. China*

²*College of Environment, Hohai University,
Nanjing 210009, P.R. China*

Abstract

To study the changes in hydration products over time during the solidification/stabilization process of magnesium potassium phosphate cementing material (MKPC) and to reveal the solidification mechanism of heavy metal elements in MKPC, methods, such as scanning electron microscope-energy spectrum (SEM-EDS), X ray diffraction (XRD), Fourier Transform Infrared Spectroscopy (FTIR) etc., were used to analyze the composition and microstructure of MKPC solidified body products with different production time, which are further adulterated with heavy metals, such as Zn, Cu, Ni, Cd and Cr, as well as changes in phases of hydration products. The results showed that the preliminary, intermediate and the final hydration products were $\text{MgHPO}_4 \cdot 7\text{H}_2\text{O}$, $\text{Mg}_2\text{KH}(\text{PO}_4)_2 \cdot 15\text{H}_2\text{O}$ and $\text{MgKPO}_4 \cdot 6\text{H}_2\text{O}$ (MKP), respectively on day 7, day 15, day 30, day 45 and day 60 after the curing of the solidified body, which was adulterated with heavy metals. Based on the analysis of the result of Cu^{2+} solidification test through FTIR, Mg^{2+} was replaced by Cu^{2+} in MKPC hydration products to generate CuKPO_4 , and the structure of the original hydration products did not have a crystal lattice change. The scanning electron microscope image (SEM) showed that cracks and harmful voids in the MKPC solidified body decreased gradually during the curing period between day 7 and day 60, and the effect of heavy metal solidification was strengthened. Based on energy spectrum analysis, heavy metal ions existing in the hydration products and MKPC could be used to solidify heavy metals. It was thus concluded that MKPC could solidify heavy metals, primarily due to the fact that heavy metals are capable of replacing Mg^{2+} . Also, they participate in a variety of chemical reactions to generate heavy metal phosphate, which could react with heavy metal ions and precipitate them. Such sediments cement and the cemented body can seal partial heavy metal ions, and the combined actions could further solidify and stabilize heavy metals.

Key Words: Magnesium Potassium Phosphate Cementing (MKPC), Heavy Metals, Solidification/Stabilization, Hydration Products

1. Introduction

In recent years, the economy in China has been

growing rapidly. Also, changing industry structure has led to the transformation of economic growth pattern from an extensive one to an intensive pattern. However, the contradiction between industrial development and environmental protection has become increasingly fierce,

*Corresponding author. E-mail: zhenshucong@163.com

and many enterprises lack environmental protection knowledge, and the potential damages to the environment are increased. Industrial pollution incidents also occur frequently across the country. According to relevant statistics, approximately 12,000,000 tons of grain in China are contaminated by heavy metals each year, which could lead to a direct economic loss of more than twenty billion Chinese yuan [1]. Furthermore, heavy metal contamination incidents in 2009 caused elevated blood lead levels over four thousand and twenty-five people, which went beyond the allowable standard of 100 µg/L. Also, elevated blood cadmium levels over one hundred and eighty-two people exceeded human body's average tolerable level of 10 µg/L, and thus triggered 32 mass disorders. Actually, data regarding a high-level forum on food safety in China showed that 1/6 of the cultivated land in China was polluted by heavy metals, with the total area of such polluted soil as more than 20,000,000 hectares in 2009. With China's rapid economic growth and subsequent improvements in the standard of living, food safety and ecological sustainability have become very important issues.

The control of heavy metal pollution incidents via engineering, biological, chemical and agricultural approaches is of theoretical and practical significance. As a mature method for solid waste treatment solidification/stabilization (s/s) has been widely applied. For example, s/s has been successfully applied in hazard-free treatment, radioactive waste recycling practice, the cleanup of bottom mud in polluted rivers, and the treatment of industrially contaminated soil, as well as hazardous solid waste with heavy metal content [2–5]. Compared with other techniques, the s/s technique is an efficient approach with wide applicability and satisfactory effect. However, organics could affect solidification strength and chemical stability, and further could cause damage to the solidified body when the wastes containing organic pollutants are treated with cement and pozzolanic materials. For this reason, researchers have strived to develop a new coagulant [6] for the treatment of organic waste, and to develop new technologies for effective solidification/stabilization of hazardous heavy metal wastes.

The chemical binding force between waste and coagulating agent, or, in other words, the force between

physical absorption of hydration products by coagulating agent and physical encapsulation of waste by coagulating agent [7–9] has often been demonstrated as the main curing mechanism of solidification/stabilization process. The main hydration product of MKPC is $\text{MgKPO}_4 \cdot 6\text{H}_2\text{O}$ (MKP) with potassium phosphate replaced to generate magnesium potassium phosphate cement [10]. Also, after added to the curing agent, chloride ions could help solidify and generate Friedel's salt [11], and the increase of solidification intensity is due to the fact that chloride ions could react with C_3A within the cement clinker to generate Friedel's salt [12]. The cementation of hydration products is the main effect of the cement solidification intensity, with the latter further affected by the output of the hydration products in the voids of the solidified body [13]. The curing mechanism for the combined use of the curing agent containing chloride ions and cement-like curing agent is that chloride ions could react with a certain component of the cement to generate Friedel's crystal salt ($\text{C}_3\text{ACaCl}_2 \cdot 10\text{H}_2\text{O}$) for solidification purpose. By using electron microscope scanning (SEM), X-ray diffraction (XRD) and relevant theoretical analysis, Bao et al. studied the performance and micro-structure of the fly-ash-flushed-by-seawater binding material adulterated with chlorine salt [14]. They found that the chlorine salt would solidify, and the increase of the binding intensity was mainly due to the fact that the fly-ash-flushed-by-seawater binding material adulterated with chlorine salt would solidify and generate Friedel's salt. However, the long-term behaviour and definite encapsulation mechanism of solidified bodies under different chemical environments have not been fully recognized yet. For example, when an encapsulated body is damaged, released heavy metals might contaminate the environment again and thus result in unforeseeable negative effects [15]. Overall, the curing mechanisms and solidification products of new-type magnesium phosphate group cementing materials are still in the preliminary research stage, and the main objective of the current research is to identify and disclose the causes of the solidification/stabilization process of heavy metals by MKPC based on a combination of analytical investigations and practical approaches such as SEM-EDS, XRD and FTIR.

2. Material and Methods

2.1 Material

1. Dead Burnt Magnesium Oxide

The magnesite used for preparing MKPC in the current research was produced by Liaoning Hengren Dongfanghong hydropower station magnesite plant. It was obtained by the grinding and high-temperature processing of magnesite (i.e., over 1500 °C). The used magnesite was Class DM-3, and the content of magnesium oxide was greater than eighty-four percent. The remaining constituents included Al₂O₃ (2.3%), SiO₂ (9.4%), CaO (2.6%), MnO (0.1%) and Fe₂O₃ (1.6%) with an average grain size of 19.9 μm.

2. Analytical reagents were used for monopotassium phosphate, borax, zinc nitrate, nickel nitrate, chromic nitrate, cupric nitrate, cadmium nitrate and so on.

2.2 Methods

1. Preparation of magnesium potassium phosphate cement (KPMC) containing heavy metals

The base mix proportions of MKPC slurry were nMgO:nMPP = 5:1, mNB:mMgO = 10%, W/C = 0.1, m MgO:mW = 5:1.

Note: Monopotassium phosphate (MPP), sodium borate (NB), W-water, C-cement (solid), n:n is molar ratio, m:m is mass ratio.

The heavy metal was added to the above mixture as per 1 g/kg, which was then mixed well immediately after the addition of water, placed in a cement curing box at a temperature of 20 ± 1 °C, and cured for day 7, day 15, day 30, day 45 and day 60 at humidity conditions (i.e., greater than ninety-five percent humidity).

2. SEM-EDS Analysis

The cement specimen at a specific age was adhered to the copper specimen holder with conductive tape, which was then placed in the scanning electron microscope after vacuum metallizing process, and the microscopic morphology of the cement hydration products was observed. An energy spectrometer was used in conjunction with the scanning electron microscope in order to analyze the type and content of micro area composition elements in the magnesium potassium phosphate cement.

3. XRD Analysis

The X-ray diffractometer was used to analyze the phase composition of the MKPC sample (tube voltage 40 kV, tube current 100 mA, slit DS = SS = 1°, RS = 0.3 mm, step length 0.05/step, scanning speed 10/min). Cement hydrated specimens at various ages were placed into an agate mortar, levigated, and screened by a square hole screen with a mesh size of 0.08 mm. They then were analysed based on X-ray diffraction. The mortar was always cleaned with dilute acid before and after every complete grinding process of the specimen.

4. FTIR Analysis

1–2 mg sample and 200 mg dry potassium bromide crystal (powder) were collected and ground into well-mixed fine powder (particle size of approximately 2 μm) in an agate mortar, which were then loaded into the mould and pressed into flakes in an oil press for further test.

3. Results

3.1 Cu Solidification in MKPC Hydration Product Phase

To study changes in solidification products of heavy metals in MKPC, only a heavy metal, copper, was added to the solidified body. The morphology of the hydration products was analyzed and observed using SEM-EDS, and a component analysis was conducted around the micro areas. In the meantime, 5 graphs representing different hydration ages, namely, day 7, day 15, day 30, day 45 and day 60, were selected for analysis. See Figure 1 for SEM-EDS diagram. See Table 1 for analytical data on the energy spectrum of hydration product phases.

Copper element was present in the hydration products around the micro areas (graph 1, graph 3 and graph 4) in Figure 1. This indicated that copper element did exist in hydration products. The MKPC could help solidify heavy metals in the crystal lattice of hydration products, and thus the solidification behavior could be displayed. In Table 1, the SEM-EDS enabled the quantitative analysis regarding specific point and region of the sample. In terms of such analyzed specific point, the credibility of component analysis was very high, but such point could not represent other analyzed materials ex-

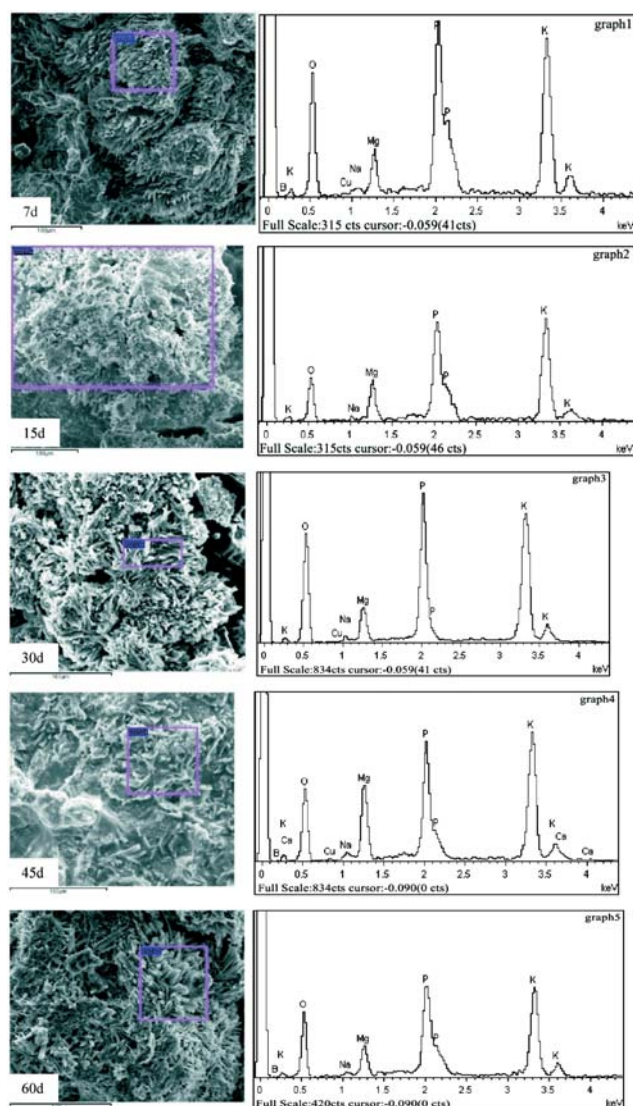


Figure 1. Different curing periods of MKPC hydration products using SEM-EDS.

cept for the detection of micro zone. The curing time of samples 1–5 was 7 d, 15 d, 30 d, 45 d and 60 d, respectively. The specific points that were analyzed by SEM-EDS corresponded to different points that went beyond curing time, which did not represent the measure result of identical materials with different curing time, leading to copper factor in sample 2 and sample 5 in Table 1. There were 3 points where copper could be detected copper, and these 3 points represent different curing time points that could be used to help explain some existing problems. As a result, there is no much improvement in the experiment.

In Figure 1 graph 1, the acicular crystal is long and thin. Both Table 1 and graph 1 represents the relative proportion of various factors. P could bind with Mg, Cu, K, Na and other elements to form compound XRD spectrogram and quantitative analysis of elements using SEM-EDS could help ascertain the molecular formula of compound $\text{MgHPO}_4 \cdot 7\text{H}_2\text{O}$, a preliminary hydration product. In graph 2, there is little crystalline which might be MgO . Because the main components of this material consist of MgO and KH_2PO_4 , the final product after chemical reactions is $\text{MgKPO}_4 \cdot 6\text{H}_2\text{O}$. According to the relationship between reactants and products, $n\text{MgO}:n\text{MPP}$ should be 1:1. In this paper, $n\text{MgO}:n\text{MPP} = 5:1$ indicating MgO is much more excessive. If there is no much crystal generated by SEM, it should primarily be MgO instead of completely hydrated or other raw materials. In graph 3, on the other hand, the crystal is thicker and bigger than that of graph 1, exhibiting a prismatic shape, with $\text{Mg}_2\text{KH}(\text{PO}_4)_2 \cdot 15\text{H}_2\text{O}$ as an intermediate hydration product. Graph 4 displays lamellar and $\text{MgKPO}_4 \cdot 6\text{H}_2\text{O}$ with

Table 1. MKPC hydration products EDS data

graph	percentage	B K	O K	Na K	Mg K	P K	K K	Cu K	Ca K
1	Wt%	44.98	34.17	0.29	2.23	6.95	11.27	0.11	
	At%	60.17	30.89	0.18	1.33	3.25	4.17	0.03	
2	Wt%	53.62	23.84	0.09	3.07	7.16	12.22		
	At%	69.62	20.92	0.06	1.77	3.25	4.39		
3	Wt%	30.20	41.75	0.41	2.65	11.22	13.68	0.09	
	At%	44.75	41.79	0.29	1.74	5.80	5.60	0.02	
4	Wt%	37.32	32.79	0.53	5.90	8.66	14.03	0.17	0.61
	At%	53.74	31.91	0.36	3.78	4.35	5.58	0.04	0.24
5	Wt%	50.04	30.13	0.32	2.32	6.42	10.76		
	At%	65.16	26.51	0.20	1.35	2.92	3.87		

a higher content of copper element in comparison with previous hydration products. Based on the content of Cu^{2+} during the hydration product phase in Figure 1 and Table 1, Cu^{2+} must have been well solidified during the preliminary and intermediate hydration product phases.

3.2 Analysis of Solid Phase Composition During the MKPC Hydration Process

Cu, Zn, Ni, Cd and Cr were added. Figure 2 represents the XRD graph of the solidified body during different hydration stages.

In Figure 2, characteristic peaks of $\text{MgHPO}_4 \cdot 7\text{H}_2\text{O}$ and $\text{Mg}_2\text{KH}(\text{PO}_4)_2 \cdot 15\text{H}_2\text{O}$ were present in XRD, and the peak value of $\text{MgHPO}_4 \cdot 7\text{H}_2\text{O}$ was higher than the peak value of $\text{Mg}_2\text{KH}(\text{PO}_4)_2 \cdot 15\text{H}_2\text{O}$ when MKPC hydration stage reached day 7, which indicated that $\text{MgHPO}_4 \cdot 7\text{H}_2\text{O}$ was the primary product [16,17]. When the hydration stage reached day 15, the peak of $\text{MgHPO}_4 \cdot 7\text{H}_2\text{O}$ disappeared completely, whereas only the peak of $\text{Mg}_2\text{KH}(\text{PO}_4)_2 \cdot 15\text{H}_2\text{O}$ existed. In the meantime, a small peak of MKP appeared, although the peak value of $\text{Mg}_2\text{KH}(\text{PO}_4)_2 \cdot 15\text{H}_2\text{O}$ started to decrease gradually until it completely disappeared after day 30. On day 30, significant MKP characteristic peak appeared, which indicated that the main MKPC hydration product was MKP, and both $\text{MgHPO}_4 \cdot 7\text{H}_2\text{O}$ and $\text{Mg}_2\text{KH}(\text{PO}_4)_2 \cdot 15\text{H}_2\text{O}$ had been hydrated and transformed into MKP. When the hy-

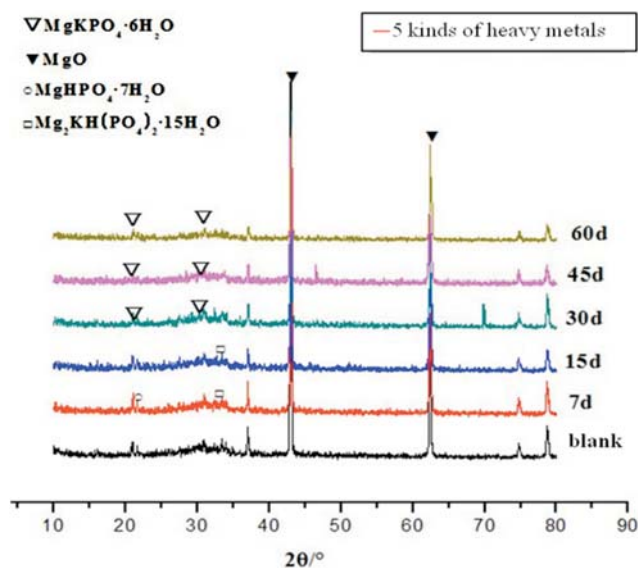


Figure 2. MKPC solidified body XRD during different hydration stages.

dration stage reached day 45, the number of MKP hydration products increased somehow, and MKPC was continuously hydrated. On day 60, the peak value of MKP was very high, indicating that the dominant final hydration product was MKP.

3.3 Changes in Microcosmic Morphology During MKPC Hydration Process

The SEM image of the solidified MKPC body, which was adulterated with the addition of Cu, Zn, Ni, Cd and Cr after the curing process (Figure 3).

It can be seen from Figure 3 that a number of acicular crystals exist in the sample on day 7 after curing the intersect and overlap. Also, a number of prismatic crystals could disperse around the whole areas in the sample on day 15 after the curing process, with the hydration crystals grown up and connected. In the meantime, a certain quantity of acicular crystals could still be observed, and a number of cracks and defects could be found among

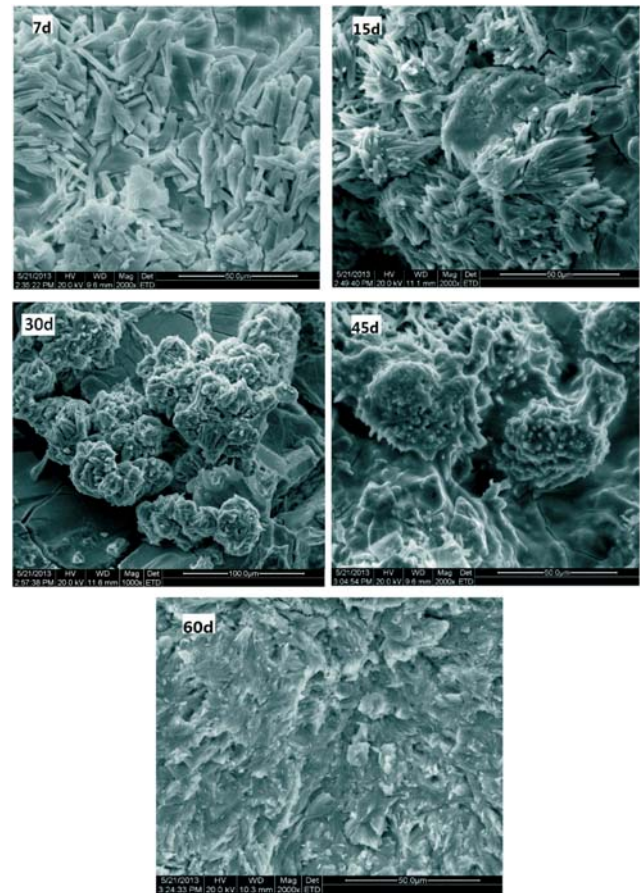


Figure 3. MKPC SEM during different hydration stages.

crystals. The crystal substance became lamellar and a number of crystals aggregated on day 30 after the curing process. After day 45, however, the crystals cemented together, and the number of voids decreased, leading to compact structure over time. The hydration products of the specimen were connected together and distributed uniformly. By contrast, the crystals grew larger and became more complete on day 60 after the curing process.

3.4 Structural Analysis of MKPC Hydration Products

The infrared spectrograms for MKPC solidified body adulterated with the addition of Cu, Zn, Ni, Cd and Cr after curing for day 45 and day 60 (Figures 4 and 5).

Based on the contrast between the one with a 45-day curing period and the blank sample, the peak shapes were basically the same. Also, the intensity of the absorption band changed somewhat, although it was still equal to the blank sample, and there was no any new band generated. It could be seen from the results that the absorption peaks were more likely to be displaced after the reactions between MKPC and heavy metals, indicating that a coordination reaction had occurred (i.e., between Mg-O and MKPC). Also, heavy metal ions, as well as a stable complex, have been generated.

Taking the infrared spectrogram of the solidified body cured for day 60, an analysis was conducted with the structural radicals corresponding to various bands as shown in Figure 5. The corresponding peak of 3400 cm^{-1} was very sharp (located at $3645\text{--}3300\text{ cm}^{-1}$) and thus represented the stretching absorption band of hydroxide radicals found in the crystal water. The corresponding peak of $1320\text{--}1105\text{ cm}^{-1}$ was the stretching vibration

band of P-O. The corresponding peak of 559 cm^{-1} was the absorption band of Mg-O bond. We ascertained the molecule formula of the final product $\text{MgKPO}_4 \cdot 6\text{H}_2\text{O}$ using infrared spectrum analysis, combining the known material proportioning, and checked a multi-spectrum retrieval technique [18,19].

4. Discussion

4.1 Effects of Curing Time on the Solidification of Heavy Metals

It can be seen from the SEM image shown in Figure 1 that the morphology of MKPC hydration products evolves from initial acicular to prismatic and finally into lamellar. In the meantime, the structure becomes more compact and the number of cracks keeps decreasing with prolonged hydration period, indicating that the solidification effect imposed by MKPC on heavy metals becomes more significant, and a stable substance is generated accompanying such prolonged period. The diffraction peak of MgO in the XRD spectrogram of MKPC (Figure 2) is very strong, indicating that the cement hydration is initially incomplete. However, with prolonged hydration period, MKP is generated with such high amount of crystalline phase. Also, the intensity of the diffraction peak increases with the prolonged curing time to some extent, indicating that the crystals of the hydration phase would keep increasing with prolonged curing time. It can be seen from the spectrogram that with curing time between day 7 and day 60 (Figure 2), the MKPC hydration product is acicular $\text{MgHPO}_4 \cdot 7\text{H}_2\text{O}$ at the early stage, prismatic $\text{Mg}_2\text{KH}(\text{PO}_4)_2 \cdot 15\text{H}_2\text{O}$ at the

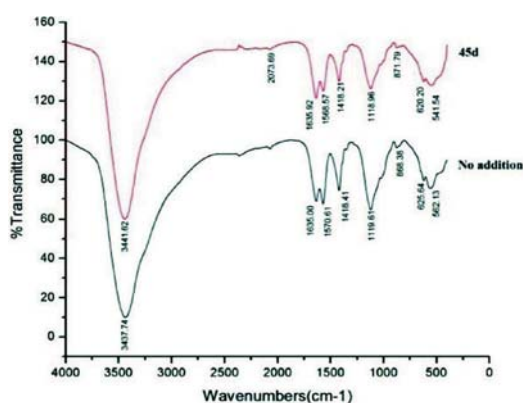


Figure 4. Curing 45 day and blank infrared spectrogram.

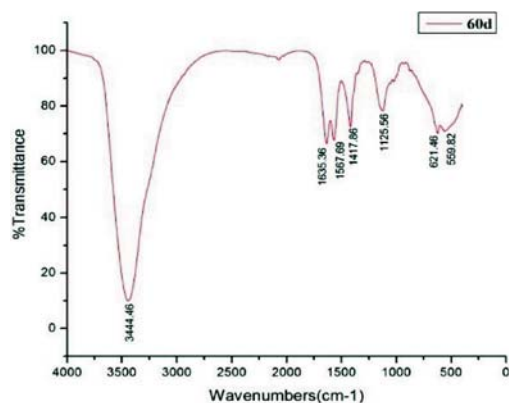


Figure 5. Curing 60 day MKPC infrared spectrogram.

intermediate stage and the final stable lamellar hydration product is $\text{MgKPO}_4 \cdot 6\text{H}_2\text{O}$. The evolution process of the products is also a process where the solidified body tends to become stable with increasing intensity. The intensity of the main diffraction peak of MgO decreases significantly, indicating that the hydration of MgO takes place gradually, and more MKP crystals would be generated with prolonged curing time. As a result, the solidification effect on heavy metals becomes stronger with a prolonged curing time. For example, based on SEM-EDS analysis on the separately solidified Cu body in Table 1, Cu^{2+} exists in the hydration product, which indicates that the crystal substance of copper is generated, and the solidification effect on Cu^{2+} is imposed by MKPC. As a result, Cu^{2+} tends to become concentrated during the preliminary and intermediate phases of the hydration product. In addition, based on the XRD analysis, $\text{CuKPO}_4 \cdot 6\text{H}_2\text{O}$ is generated, and other heavy metals could also generate crystals containing $6\text{H}_2\text{O}$, and such heavy metals could also be solidified just as Cu^{2+} . Evidently, the prolongation of the curing time is significant in increasing the strength of the solidified body and enhancing the solidification effect on heavy metals.

4.2 The Analysis of Curing Mechanism

Present studies generally consider that the main mechanisms of waste solidification/stabilization by MKPC stabilization technology include the chemical binding forces between waste and coagulating agents, physical absorption of hydration products by coagulating agents, and physical encapsulation of waste by coagulating agents [7,15,16]. Heavy metal ions may be solidified in the hydration products by means of adsorption, co-existence and the chemical replacement of interlayer positions among others. Rao et al. have shown that pollution elements are often converted into relevant phosphates with low solubility through chemical reactions in order to solidify and stabilize such pollution elements [12]. Singh et al. have found that heavy metals might be further encapsulated into the substrate of magnesium potassium phosphate cement after heavy metal phosphate with low solubility is generated [17]. Even for the same heavy metal element, the solubility of its phosphate product is generally lower than that of its hydroxide [18]. Compared with hydroxide, phosphate can adapt to a

wider range of pH, and thus becomes more stable after the solidification process. The formed magnesium phosphate substrate eventually becomes stable in the ambient environment. Magnesium potassium phosphate might further prevent the leaching of the contaminants in the solidified body after the heavy metal is encapsulated, with its solubility as solely 2.4×10^{-11} .

The confidence level of the acquired results is low, partly due to the limitation of the test method. Although some studies have studied the mechanism of solidification effect on heavy metals imposed by phosphate base cementing materials, definite encapsulation mechanism and clear understanding of the long-term behavior of the solidified body in different chemical environments remains insufficient, let alone the encapsulation mechanism. Hazardous components will re-enter the environment and cause unforeseeable effects when the encapsulation body ruptures. Therefore, it is necessary to further discuss effective detection or test methods, and explore the curing mechanism of heavy metal ions in the solidified body.

Based on an analysis of Figures 1 and 2, the preliminary MKPC hydration product is acicular $\text{MgHPO}_4 \cdot 7\text{H}_2\text{O}$, the intermediate MKPC hydration product is prismatic $\text{Mg}_2\text{KH}(\text{PO}_4)_2 \cdot 15\text{H}_2\text{O}$, and the final MKPC hydration product is lamellar $\text{MgKPO}_4 \cdot 6\text{H}_2\text{O}$. It can be seen from the morphological changes that the structure of the solidified body becomes more compact, and the cracks diminish with prolonged curing time. In addition, after dissolution of monopotassium phosphate, $\text{MgHPO}_4 \cdot 7\text{H}_2\text{O}$ is first precipitated and then changed into $\text{Mg}_2\text{KH}(\text{PO}_4)_2 \cdot 15\text{H}_2\text{O}$ until eventually it becomes $\text{MgKPO}_4 \cdot 6\text{H}_2\text{O}$ at the final stage of the reaction process. Based on the analysis on Table 1, a coordination reaction occurs between MKPC Mg-O and Cu^{2+} , and a stable complex $\text{CuKPO}_4 \cdot 6\text{H}_2\text{O}$ is generated. It is thus evident that other heavy metals could generate stable phosphate crystals containing six water molecules, and thus enable solidification and stabilization of heavy metals the same way as Cu does.

Based on the above analysis, the mechanism of solidification on heavy metals imposed by MKPC can be stated as follows: as the pH of MKPC slurry exhibits alkalescence, heavy metals are capable of substituting for Mg^{2+} and participating in following reactions in order to generate heavy metal phosphate. As a result, heavy metal ions are converted to non-dissolvable sediments.

Since such sediments cement and the cemented body can further seal partial heavy metal ions, the combined actions could solidify and stabilize heavy metals.

5. Conclusions

In the present study, MKPC cement solidified body is adulterated with Cu, Zn, Ni, Cd and Cr. Separately, it is specifically adulterated with Cu and cured for day 7, day 15, day 30, day 45 and day 60. XRD is used to analyze the phase of the hydration products of solidified MKPC body. SEM-EDS is then used to analyze the morphological, compositional and structural characteristics of hydration products. Finally, FTIR is used to analyze the material structure of hydration products. A comprehensive analysis is further conducted in order to reveal the type, morphology, composition and structure formation process of MKPC hydration system products, and to ascertain the mechanism of solidification effect on heavy metals imposed by MKPC. Based on such series analyses, the following conclusions could be drawn:

- (1) The preliminary MKPC hydration product is acicular $\text{MgHPO}_4 \cdot 7\text{H}_2\text{O}$, the intermediate one is prismatic $\text{Mg}_2\text{KH}(\text{PO}_4)_2 \cdot 15\text{H}_2\text{O}$, and the final one is lamellar $\text{MgKPO}_4 \cdot 6\text{H}_2\text{O}$. It can be seen from the SEM spectrogram that the structure of the solidified body is compact. Also, with prolonged hydration period, the cracks begin to diminish, and the products would change continuously. The energy spectrum and XRD analysis demonstrates that Cu^{2+} exists in the hydration products, with CuKPO_4 as a generated product, which would further enable the solidification/stabilization process of heavy metals.
- (2) The mechanism analysis shows that heavy metals are capable of substituting for Mg^{2+} and participating in the following reactions in order to generate heavy metal phosphate. As a result, heavy metal ions could form non-dissolvable sediments. Such sediments cement and the cemented body can seal partial heavy metal ions, and the combined actions could further solidify and stabilize heavy metals.

Acknowledgements

This work was supported by the Ministry of Housing

and Urban-Rural Development of the People's Republic of China research and development projects (2012-K4-21) and China Building Materials Industry Association technology innovation projects (2013-M5-2).

References

- [1] Yang, S. C., Nan, Z. R. and Zeng J. J., "Current Situation of Soil Contaminated by Heavy Metals and Research Advances on the Remediation Techniques," *Journal of Anhui Agriculture Science*, Vol. 34, No. 3, pp. 549–552 (2006).
- [2] Malviya, R. and Chaudhary, R., "Factors Affecting Hazardous Waste Solidification/Stabilization: A Review," *Journal of Hazardous Materials*, Vol. 137, No. 1, pp. 267–276 (2006). doi: 10.1016/j.jhazmat.2006.01.065
- [3] Conner, J. R., *Chemical Fixation and Solidification of Hazardous Wastes*, Van Nostrand Reinhold New York Press, New York, pp. 102–122 (1990).
- [4] Barth, E. F., Percin, P. D. and Arozarena, M. M., *Stabilization and Solidification of Hazardous Wastes*, Noyes Publications, New York, pp. 12–68 (1990). doi: 10.1520/STP19568S
- [5] Barth, E. F., "An Overview of the History, Present Status, and Future Direction of Solidification/Stabilization Technologies for Hazardous Waste Treatment," *Journal of Hazardous Materials*, Vol. 24, No. 2, pp. 103–109 (1990). doi: 10.1016/0304-3894(90)87002-Y
- [6] Josephson, J., "Immobilization and Leachability of Hazardous Wastes," *Environ. Sci. Technol (United States)*, Vol. 16, No. 4, (1982). doi: 10.1021/es00098a720
- [7] Cheng, K. Y., Bishop, P. and Isenburg, J., "Leaching Boundary in Cement-Based Waste Forms," *Journal of Hazardous Materials*, Vol. 30, No. 3, pp. 285–295 (1992). doi: 10.1016/0304-3894(92)87005-Z
- [8] Ye Cheng, K. and Bishop, P. L., "Developing a Kinetic Leaching Model for Solidified/Stabilized Hazardous Wastes," *Journal of Hazardous Materials*, Vol. 24, No. 2, pp. 213–224 (1990). doi: 10.1016/0304-3894(90)87011-6
- [9] Lin, C., Lin, T. and Huang, T., "Leaching Processes of the Dicalcium Silicate and Copper Oxide Solidification/Stabilization System," *Toxicological & Environ-*

- mental Chemistry*, Vol. 44, No. 1–2, pp. 89–100 (1994). doi: [10.1080/02772249409358047](https://doi.org/10.1080/02772249409358047)
- [10] Wagh, A. S. and Singh, D., *Method for Stabilizing Low-Level Mixed Wastes at Room Temperature*, Google Patents (1997).
- [11] Graeser, S., Postl, W., Bojar, H., et al., “Struvite-(K), $\text{KMgPO}_4 \cdot 6\text{H}_2\text{O}$, the Potassium Equivalent of Struvite - A New Mineral,” *European Journal of Mineralogy*, Vol. 20, No. 4, pp. 629–633 (2008). doi: [10.1127/0935-1221/2008/0020-1810](https://doi.org/10.1127/0935-1221/2008/0020-1810)
- [12] Rao, A. J., Pagilla, K. R. and Wagh, A. S., “Stabilization and Solidification of Metal-Laden Wastes by Compaction and Magnesium Phosphate-Based Binder,” *Journal of the Air & Waste Management Association*, Vol. 50, No. 9, pp. 1623–1631 (2000). doi: [10.1080/10473289.2000.10464193](https://doi.org/10.1080/10473289.2000.10464193)
- [13] Huang, X., “Strength Enhancement Effect of ET2 Tringite in Soil Stabilization,” *Journal of the Chinese Ceramic Society*, Vol. 28, No. 4, pp. 299–302 (2000).
- [14] Bao, L. S., Song, X. C., Yu, L. and Wang, H. J., “Study on Bonding Mechanism of Chloride in the Cement Sea-Fly-Ash Binder,” *Journal of Shenyang Jianzhu University (Natural Science)*, Vol. 26, No. 1, pp. 36–40 (2010).
- [15] Roy, A., Eaton, H. C., Cartledge, F. K. and Tittlebaum, M. E., “Solidification/Stabilization of Hazardous Waste: Evidence of Physical Encapsulation,” *Environmental Science & Technology*, Vol. 26, No. 7, pp. 1349–1353 (1992). doi: [10.1021/es00031a011](https://doi.org/10.1021/es00031a011)
- [16] Qin, L. Q., Xie, J. R., Zhang, H. and Dong, W. L., “Real Time Analysis of Hydration Process of Calcium Phosphate Bone Cement by XRD,” *Journal of Instrumental Analysis*, Vol. 19, No. 3, pp. 68–70 (2000).
- [17] Huang, C. M., Zhang, Q., Bai, S. and Wang, C. S., “FTIR and XRD Analysis of Hydroxyapatite from Fossil Human and Animal Teeth in Jinsha Relict, Chengdu,” *Spectroscopy and Spectral Analysis*, Vol. 27, No. 12, pp. 2448–2452 (2008).
- [18] Mariey, L., Signolle, J. P., Amiel, C. and Travert, J., “Discrimination, Classification, Identification of Microorganisms Using FTIR Spectroscopy and Chemometrics,” *Vib. Spectrosc.*, Vol. 26, No. 2, pp. 151–159 (2001). doi: [10.1016/S0924-2031\(01\)00113-8](https://doi.org/10.1016/S0924-2031(01)00113-8)
- [19] Ning, Y. C., *Structural Identification of Organic Compounds and Organic Spectroscopy*, Science Press, Beijing, pp. 322–355 (2002).
- [20] El-Jazairi, B., “Rapid Repair of Concrete Pavings,” *Concrete*, Vol. 16, No. 9, pp. 12–15 (1982).
- [21] Singh, D., Wagh, A. S., Cunnane, J. C. and Mayberry, J. L., “Chemically Bonded Phosphate Ceramics for Low-Level Mixed-Waste Stabilization,” *Journal of Environmental Science & Health Part A*, Vol. 32, No. 2, pp. 527–541 (1997). doi: [10.1080/10934529709376559](https://doi.org/10.1080/10934529709376559)
- [22] Dean, J. A., *Lange’s Chemistry Handbook*, McGraw-Hill, Inc, New York, pp. 35–112 (1999).

Manuscript Received: May 5, 2014

Accepted: Sep. 29, 2014